Chapter 1

Field-Induced Superconductors: NMR Studies of λ–$(BETS)_2FeCl_4$

Guoqing Wu and W. Gilbert Clark

Additional information is available at the end of the chapter

http://dx.doi.org/10.5772/48361

1. Introduction

It has been widely known in condensed matter and materials physics that the application of magnetic field to a superconductor will generally destroy the superconductivity as a usual scenario. There are two reasons responsible for this.

One is the Zeeman effect [1-2], where the alignment of the electron spins by the applied magnetic field can break apart the electron pairs for a spin-singlet (but not a spin-triplet) state. In this case, the electron spin pairs have opposite spins (such as the *s*-wave spins typical in type I superconductors). The applied magnetic field attempts to align the spins of both electrons along the field, thus breaking them apart if strong enough. In terms of energy, one electron gains energy while the other (as a pair) loses energy. If the energy difference is larger than the amount of energy holding the electrons together, then they fly apart and thus the superconductivity disappears. But this does not apply to the spin triplet superconductivity (*p*-wave superconductors) where the electron pairs already have their spins aligned (along the field) in a *p*-wave state.

The other is the orbital effect [3], which is a manifestation of the Lorentz force from the applied magnetic field since the electrons (as a pair) have opposite linear momenta, one electron rotating around the other in their orbitals. The Lorentz force on them acts in opposite directions and is perpendicular to the applied magnetic field, thus always pulling the pair apart. This does not matter with their spin pairing symmetries (*s*-wave, *p*-wave or *d*-wave). In type-II superconductors, the Meissner screening currents associated with the vortex penetration in the applied magnetic field can also increase the electron kinetic energy (and momentum). Once this energy becomes greater than the energy that unites the two electrons, the electron pairs break apart and thus superconductivity is suppressed. Therefore, the orbital effect could be even more important in type-II superconductors.

However, in certain complex compounds, especially in some low-dimensional materials, superconductivity can be enhanced [4 - 5] by the application of magnetic field. The enhancement of superconductivity by magnetic field is a counter-intuitive unusual phenomenon.

In order to understand this interesting phenomenon, different theoretical mechanisms have been proposed, while there are still debates and experimental evidence is needed. The first theory is the Jaccarino-Peter compensation effect [6], the second theory is the suppression effect of the spin fluctuations [7-9], and the third theory is the anti-proximity effect (in contrary to the proximity effect [10]) found in the nanowires recently [11]. These theories will be briefly described in Section 3.

Experimentally, there are several effective techniques that can be used to the study of the superconductivity of the materials with magnetic field applications. They include electrical resistivity measurements, Nernst effect measurements, SQUID magnetic susceptibility measurements, and nuclear magnetic resonance (NMR) measurements, etc.

Among these experimental techniques, NMR is one of the most powerful ones and it is a versatile local probe capable of directly measuring the electron spin dynamics and distribution of internal magnetic field including their changes on the atomic scale. It has been widely used as a tool to investigate the charge and spin static and dynamic properties (including those of the nano particles). It is able to address a remarkably wide range of questions as well as testing the validity of existing and/or any proposed theories in condensed matter and materials physics.

The authors have extensive experience using the NMR and various other techniques for the study of the novel condensed matter materials. This chapter focuses on the NMR studies of the quasi-two dimensional field-induced superconductor λ–$(BETS)_2FeCl_4$. This is a chance to put some of the work together, with which it will help the science community for the understanding of the material as well as for the mechanism of superconductivity. It will also help materials scientists in search of new superconductors.

2. Field-induced superconductors

The discovery of field-induced superconductors is about a decade earlier than the discovery of the high-T_c superconductors (which have been found since 1986), while not many field-induced superconductors have been found. Both types of materials, field-induced superconductors and high-T_c superconductors, are highly valuable in science and engineering due to their important physics and wonderful potentials in technical applications.

Here are typical field-induced superconductors found so far, with chemical compositions as shown in the following

1. $Eu_xSn_{1-x}Mo_6S_{8-y}Se_y$, $Eu_xLa_{1-x}Mo_6S_8$, $PbGd_{0.2}Mo_6S_8$, etc.[5, 7].
2. λ–$(BETS)_2FeCl_4$, λ–$(BETS)_2Fe_xGa_{1-x}Br_yCl_{4-y}$, κ–$(BETS)_2FeBr_4$, etc.[4, 8, 9].
3. Al-nanowires (ANWs), Zinc-nanowires (ZNWs), MoGe nanowires, and Nb nanowires, etc. [10-13].

3. Theory for field-induced superconductors

In this section, we will briefly describe the theoretical aspects for the field-induced superconductors regarding their mechanisms of the field-induced superconductivity. We will mainly discuss the theory of Jaccarino-Peter effect, the theory of spin fluctuation effect, and the theory of anti-proximity effect.

3.1. Theory of Jaccarino-Peter effect

This theory was proposed by Jaccarino, V. and Peter, M. in 1962 [6]. It means that if there is an existence of localized magnetic moments at a state and conduction electrons as well at the same state in a material, then it could lead to a negative exchange interaction J between the conduction electrons and the magnetic moments when an external magnetic field ($\boldsymbol{H}$) is applied. This negative exchange interaction J is formed due to the easy alignment of the localized magnetic moments (along the external magnetic field direction) while the external magnetic field $\boldsymbol{H}$ is applied. Thus the spins of the conduction electrons will experience an internal magnetic field ($\boldsymbol{H}_J$), $H_J = J\langle S\rangle/g\mu_B$, created by the magnetic moments [proportional to the average spins (<S>) of the moments]. Here the internal magnetic field $\boldsymbol{H}_J$ is called the exchange field and the direction of the exchange field $\boldsymbol{H}_J$ is opposite to the externally applied magnetic field $\boldsymbol{H}$. This picture is sketched as that shown in Fig. 1.

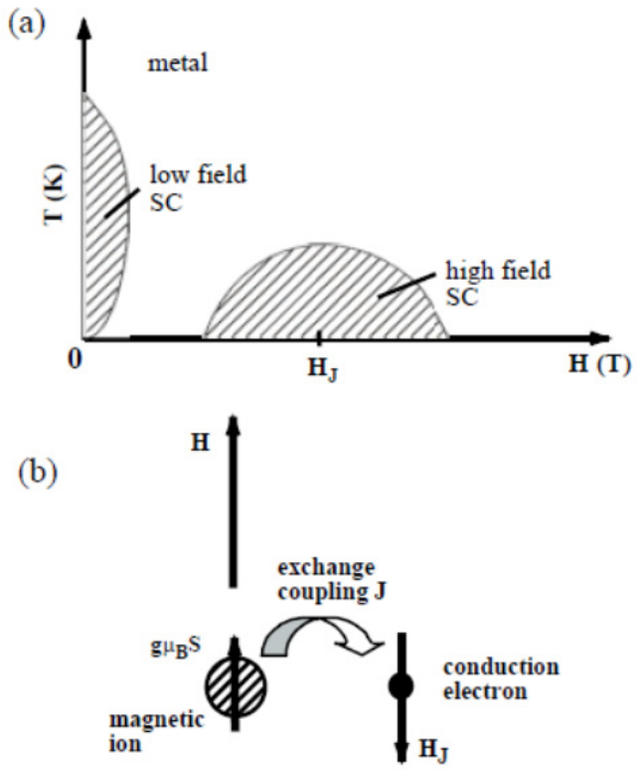

Figure 1. Schematic of Jaccarino-Peter effect [8]

In some cases, this H_J could be very strong. Therefore, if the exchange field $\boldsymbol{H}_J$ is strong enough to cancel the externally applied magnetic field $\boldsymbol{H}$, i.e., $\boldsymbol{H}_J = -\boldsymbol{H}$, then the resultant

field in total that the conduction electron spins experience becomes zero (also a complete suppression of the Zeeman effect), and thus the superconductivity is induced in this case.

Certainly, superconductivity could also be possible in this case (as a stable phase), even if without the external field $\boldsymbol{H}$ (i.e. $\boldsymbol{H} = 0$). This is because the magnetic moments point to random directions (without $\boldsymbol{H}$) and cancel each other, i.e., $\boldsymbol{H}_J = 0$, and thus the conduction electron spins also feel zero in total field.

3.2. Theory of spin fluctuation effect

This theory was mainly reported by Maekawa, S. and Tachiki, M. [7] in 1970s, with the discovery of field-induced superconductors $Eu_xSn_{1-x}Mo_6S_{8-y}Se_y$. These types of materials have rare-earth 4f-ions and paired conduction electrons from the 4d-Mo-ions. The rare-earth 4f-ions have large fluctuating magnetic moments, while the conduction electrons from the 4d-Mo-ions have strong electron–electron interactions and they form Cooper pairs.

Without externally applied magnetic field ($\boldsymbol{H} = 0$), the fluctuating magnetic field from the rare-earth 4f-ion moments at the 4d-Mo conduction electrons are so strong that it weakens the BCS coupling of the Mo-electrons. Thus there is no superconductivity without externally applied magnetic field.

However, when external magnetic field is applied ($\boldsymbol{H} \neq 0$) it suppresses the spin fluctuation, causing an increase of the BCS coupling among the conduction electrons. Thus, superconductivity appears in the presence of an applied magnetic field. This scenario can be seen from a typical *H-T* phase diagram shown in Fig. 2.

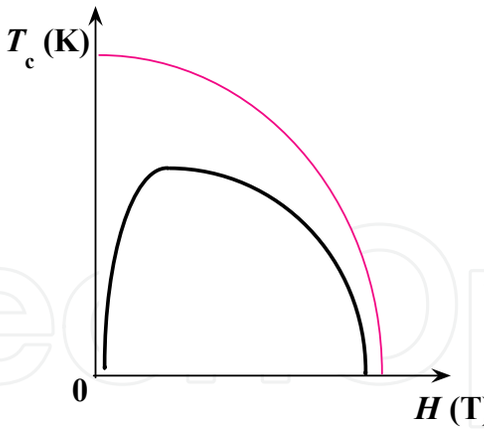

Figure 2. A possible *H-T* phase diagram for the spin fluctuation effect. The thin-red line represents a case without local spin fluctuation moments as a reference.

3.3. Theory of anti-proximity effect

3.3.1. Superconductivity in nanowires enhanced by applied magnetic field

Unlike the bulk superconductors, a nanoscale system can have externally applied magnetic field $\boldsymbol{H}$ to penetrate it with essentially no attenuation at all throughout the whole sample.

But it has been observed that the application of a small magnetic field H can decrease the resistance in even simple narrow superconducting wires (i.e., negative magnetoresistance) [12, 13], while larger applied magnetic field H can increase the critical current (I_C) significantly [14]. These indicate an enhancement of superconductivity in nanowires by the application of magnetic field. But to understand the enhancement of superconductivity by magnetic field in nanoscale systems is very challenging currently in the science community.

3.3.2. Proximity effect

On the other hand, when a superconducting nanowire is connected to two normal metal electrodes, generally a fraction of the wire is expected to be resistive, especially when the wire diameter is smaller than the superconducting coherence length. This is called the proximity effect [10].

Similarly, when a superconducting nanowire is connected to two bulk superconducting (BS) electrodes, the combined sandwiched system is expected to be superconducting (below the T_C of the superconducting nanowire and the BS electrodes), and the superconductivity of the nanowire is then expected to be more supportive and more robust through its coupling with the superconducting reservoirs. This is also actually what is theoretically expected [15].

3.3.3. Anti-proximity effect

Contrary to the proximity effect, it has been found in 2005 [11, 16] that, in a system consisting of 2 μ long, 40 nm diameter Zinc nanowires sandwiched between two BS electrodes (Sn or In), superconductivity of Zinc nanowires is completely suppressed (or partially suppressed) by the BS electrodes when the BS electrodes are in the superconducting state under zero applied magnetic field. However, when the BS electrodes are driven normal by an applied magnetic field ($\boldsymbol{H}$), the Zinc nanowires re-enter their superconducting state at ~ 0.8 K, unexpectedly. This is called ''anti-proximity effect''.

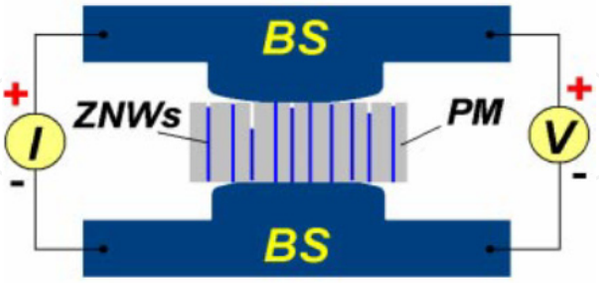

BS – bulk superconducting electrode; ZNWs – Zinc nanowires;
PM – porous membranes; I – current; V – voltage.

Figure 3. Schematic of the Zinc nanowires sandwiched between two BS electrodes [11].

This is also a counterintuitive unusual phenomenon, never reported before 2005.

The schematic of the electrical transport measurement system exhibiting the anti-proximity effect with the Zinc nanowires sandwiched between two BS electrodes is shown in Fig. 3.

3.3.4. Theory of anti-proximity effect

There are several theoretical models that could be used for the theoretical explanation of the magnetic field-induced or -enhanced superconductivity in nanowires, while some of which were proposed long before the anti-proximity effect was reported. Thus they are not generally accepted.

a. Phase fluctuation model

This model proposes that there is an interplay between the superconducting phase fluctuations and dissipative quasiparticle channels [17].

The schematic diagram of this model regarding the anti-proximity effect experiment (Fig. 3) can be re-illustrated as that shown in Fig. 4.

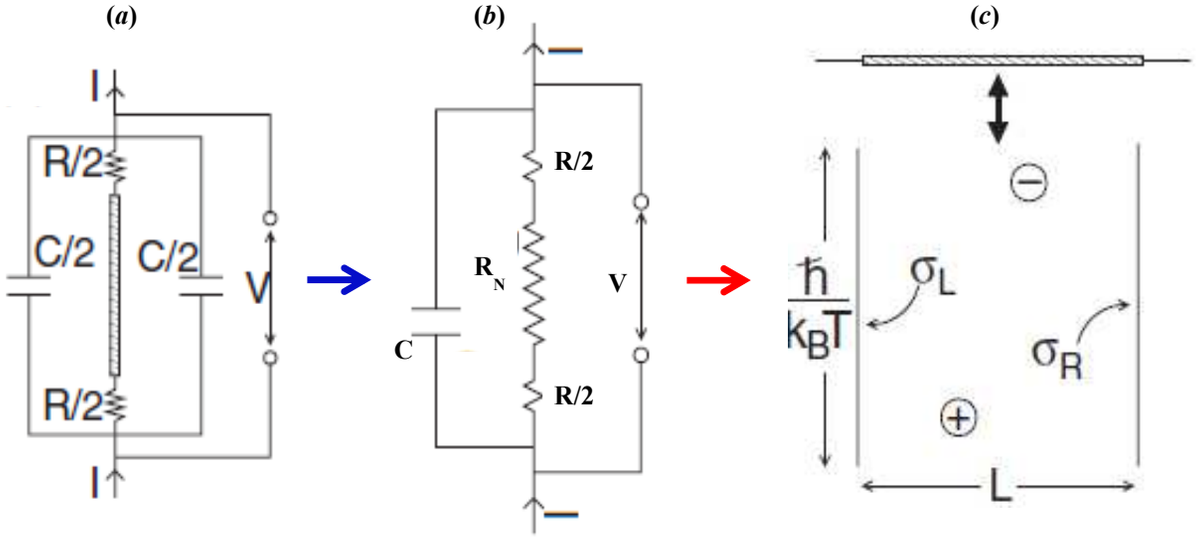

Figure 4. (a) Schematic of the anti-proximity effect experiment (Fig. 3). (b) Simplification of (a). (c) Phase fluctuations in a dissipative environment. R – resistance of the bulk electrodes, C – circuit capacitance (between the electrodes), V – voltage, I – current, σL and σR – superfluid (surface vortex densities) [17].

When the bulk electrodes are superconducting, there is a supercurrent flowing between the nanowire and BS electrodes, and the contact resistances (R) vanish (R = 0). Thus the circuit frequency becomes low, and the quantum wire is shunted by the capacitor (C) if the energy (frequency *f*) is less than the bulk superconducting gap energy of the electrodes. In this case, the quantum fluctuations of the superconducting phase drive the superfluid density (σ) of the zinc nanowire to zero (even when temperature $T = 0$). As soon as the superfluid density vanishes, the Cooper pairs dissociate and the nanowire becomes normal (with a normal resistor with resistance R_N). Thus this explains the resistive behavior at zero applied magnetic field ($H = 0$).

When the bulk electrodes are driven normal by the applied magnetic field ($H \geq 30$ mT), the contact resistances $R \neq 0$. Similarly, if the electrodes are normal but the nanowire is superconducting (or vice versa), there will be a resistance due to charge conversion processes [10]. This results in a high circuit frequency $f = 1/(2\pi RC) \sim 1$ GHz, with a behavior like a pure resistor (i.e., impedance $X_C = 1/2\pi fC \rightarrow 0$). If this shunting resistance is less the quantum of resistance ($h/4e^2 \sim 6.4$ kΩ), then it will damp the superconducting phase fluctuations, and thus stabilizing the superconductivity. On the other hand, in a dissipation environment [Fig. 4 (c)], the superfluid density (σ) of the zinc nanowire cannot screen the interaction between bulk vortices completely. As a result, the superconducting phase becomes stable for sufficiently small shunt resistance [17].

In order words, when the magnetic field is applied ($H \neq 0$) to the bulk electrodes, the dissipations between the two ends of the electrodes will be enhanced and meanwhile the superconducting phase fluctuations are damped. This leads to the stabilization of the superconductivity of the nanowires between the bulk electrodes.

b. Interference model

The interference model proposes that there is an interference between junctions of two superconducting grains, with random Josephson couplings J and J' associated with disorder, as sketched shown in Fig. 5. It produces a configuration-averaged critical current $\langle I_C \rangle$ as [18]

$$\langle I_C \rangle = \left(J^2 + J'^2\right)^{1/2} \left[1 - \frac{1}{2}\left\langle \frac{JJ'}{J^2 + J'^2} \right\rangle \cos^2\left(2\pi \frac{\Phi}{\Phi_0}\right) + \ldots \right] \quad (1)$$

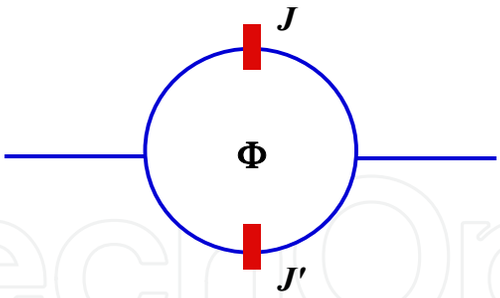

Here Φ represents for the magnetic flux through an array of each holes due to existence of disorder.

Figure 5. Schematic of interference between junctions with Josephson couplings J and J'

This is a periodic function of Φ [$\cos^2(2\pi\Phi/\Phi_0)$] with a period of half flux quantum ($\Phi_0/2 = hc/4e$), where Φ is the magnetic flux through each hole due to the existence of disorder in the sample (note, the sample has an array of holes through each of which there has a flux Φ).

Thus when Φ is small, $\langle I_C \rangle$ increases as Φ increases, and this corresponds to a negative magnetoresistance, i.e., when applied magnetic field H increases, the electrical resistivity of the nanowires drops down. Thereby the superconductivity is enhanced.

c. Charge imbalance length model

This model proposes that there is a charge-imbalance length (or relaxation time) associated with the normal metal - superconductor boundaries of phase-slip centers [20]. Applying magnetic field reduces the charge-imbalance length (or relaxation time), resulting in a negative magnetoresistance at high currents and near T_c. Thus the superconductivity in the nanowires is enhanced.

d. Impurity model

The impurity model deals with the superconductivity for nanoscale systems that have impurity magnetic moments with localized spins as magnetic superconductors [14], in which there is a strong Zeeman effect. According to this model, superconductivity is enhanced with the quenching of pair-breaking magnetic spin fluctuations by the applied magnetic field.

These are major theoretical models for the explanation of the anti-proximity effect in nanoscale systems. Their validity needs more experimental evidence.

4. Field-induced superconductor λ–$(BETS)_2FeCl_4$

The field-induced superconductor λ–$(BETS)_2FeCl_4$ is a quasi-two dimensional (2D) triclinic salt (space group P) incorporating large magnetic 3d-Fe^{3+} ions (spin S_d = 5/2) with the BETS-molecules inside which have highly correlated conduction electrons (π-electrons, spin S_π = 1/2) from the Se-ions, where BETS is bis(ethylenedithio)tetraselenafulvalene ($C_{10}S_4Se_4H_8$). It was first synthesized in 1993 by Kobayashi *et al*. [4, 8, 9, 19].

λ–$(BETS)_2FeCl_4$ is one of the most attractive materials in the last two decades for the observation of interplay of superconductivity and magnetism and for the synthesis of magnetic conductors and superconductors.

We expect it to show strong competition between the antiferromagnetic (AF) order of the Fe^{3+} magnetic moments and the superconductivity of the material, where the properties of the conduction electrons are significantly tunable by the external magnetic field, together with the internal magnetic field generated by the local magnetic moments from the Fe^{3+} ions as well. Thus it has been of considerable interest in condensed matter and materials physics.

This interplay originates from the role of the magnetic 3d-Fe^{3+} ions moments including the effect of their strong interaction with the conduction π-electrons. Because of this interplay, λ–$(BETS)_2FeCl_4$ has an unusual phase diagram [Fig. 5 (c)], including an antiferromagnetic insulating (AFI) phase, a paramagnetic metallic (PM) phase, and a field-induced superconducting (FISC) phase [4, 8].

The crystal structure of λ–$(BETS)_2FeCl_4$ in a unit cell is shown in Fig. 6 (a) [20]. In each unit cell, there are four BETS molecules and two Fe^{3+} ions. The BETS molecules are stacked along the *a* and *c* axes to form a quasi-stacking fourfold structure.

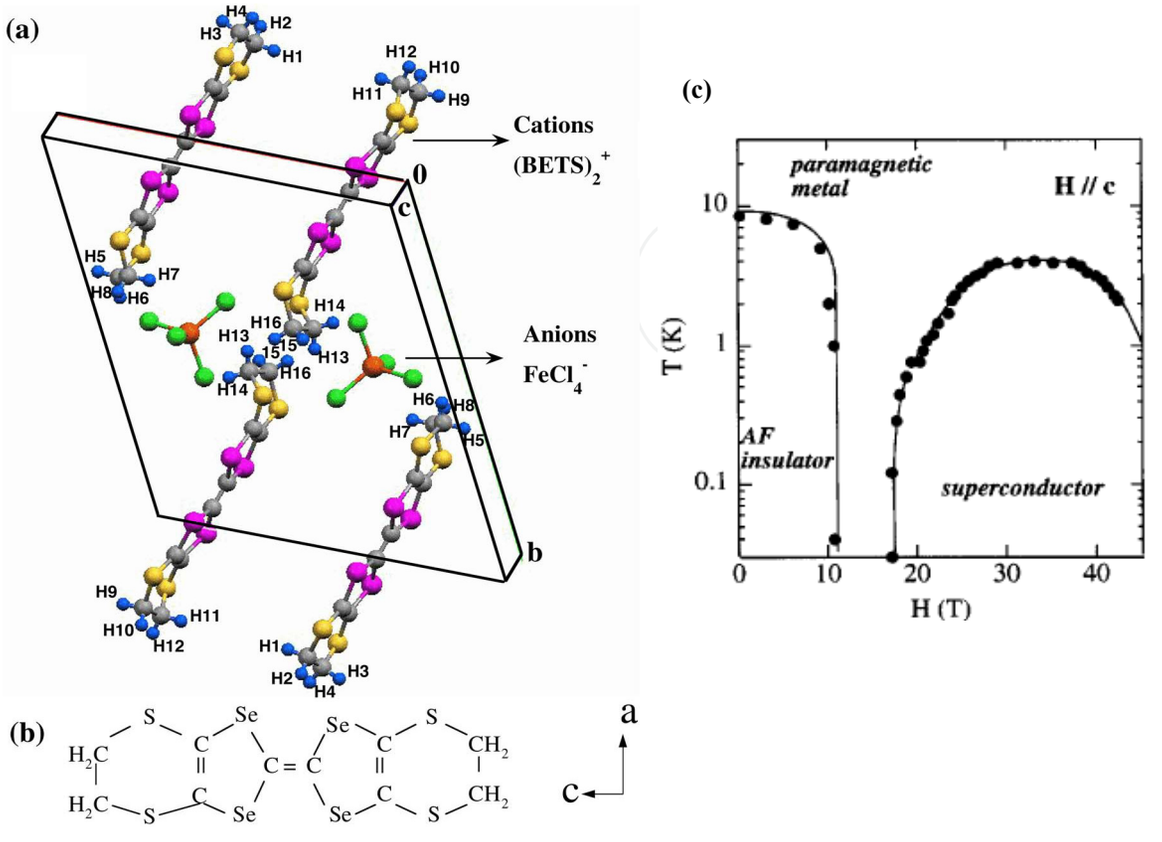

Figure 6. (a) Crystal structure of λ–(BETS)$_2$FeCl$_4$ in a unit cell. (b) BETS molecule [20]. (c) Phase diagram of λ–(BETS)$_2$FeCl$_4$ [8].

Noticeably, the conducting layers comprised of BETS are sandwiched along the *b* axis by the insulating layers of $FeCl^{4-}$ anions. The least conducting axis is *b*, the conducting plane is *ac*, and the easy axis of the antiferromagnetic spin structure is ~30° away from the *c* axis (parallel to the needle axis of the crystal) [21, 22].

At the room temperature (298 K), the lattice constants are: a = 16.164(3), b = 18.538(3), c = 6.592(4) Angstrom (A^o), α = 98.40(1)^o, β = 96.69(1)^o, and γ = 112.52(1)^o. The shortest distance between Fe^{3+} ions is 10.1 A^o within a unit cell, which is along the *a*-direction, and the nearest distance of Fe^{3+} ions between neighboring unit cells is 8.8 A^o [21].

5. NMR studies of λ–(BETS)$_2$FeCl$_4$

In order to study the mechanism of the superconductivity in λ–(BETS)$_2$FeCl$_4$ and to test the validity of the Jaccarino-Peter effect, as well as to understand the multi-phase properties of the material as show in the unusual phase diagram [Fig. 6 (c)], we successfully conducted a series of nuclear magnetic resonance (NMR) experiments.

These include both ^{77}Se-NMR measurements and proton (^{1}H) NMR measurements, as a function of temperature, magnetic field and angle of alignment of the magnetic field [20, 23, 24].

5.1. ^{77}Se-NMR measurements in λ–(BETS)$_2$FeCl$_4$

5.1.1. ^{77}Se-NMR spectrum

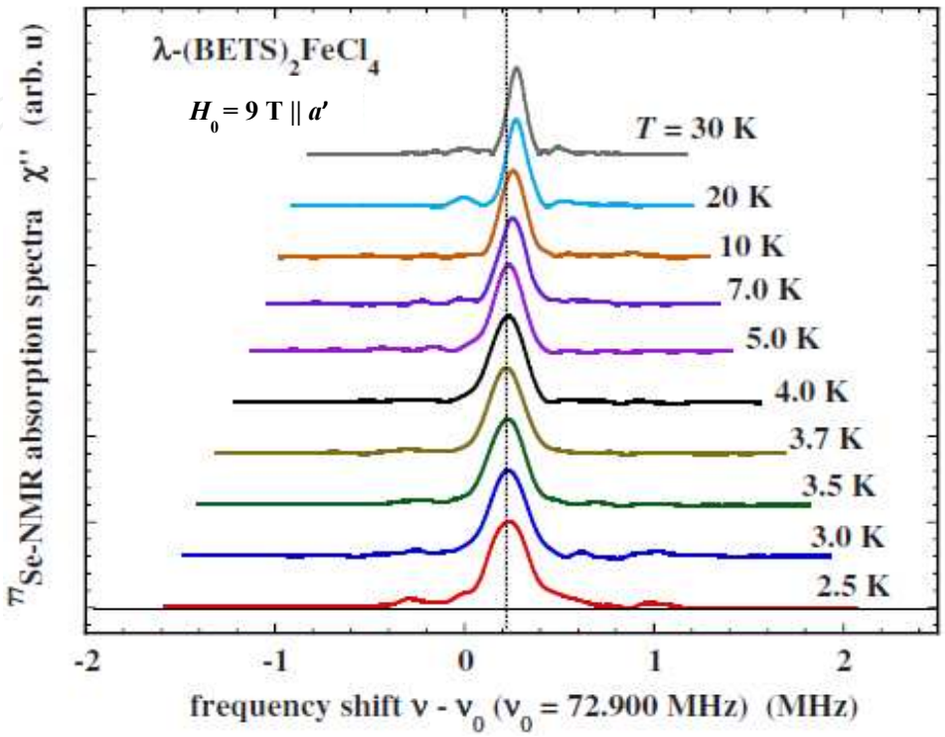

Figure 7. ^{77}Se-NMR absorption spectrum at various temperatures with applied magnetic field

H_0 = 9 T || a' in λ–(BETS)$_2$FeCl$_4$ [23].

The ^{77}Se-NMR spectra of λ–(BETS)$_2$FeCl$_4$ at various temperatures are shown in Fig. 7. The spectrum has a dominant single-peak feature which is reasonable as a spin I = 1/2 nucleus for the ^{77}Se, while it broadens inhomogeneously and significantly upon cooling (the linewidth increases from 90 kHz to 200 kHz as temperature is lowered from 30 K to 5 K). What the^{77}Se-NMR spectrum measures is the local field distribution in total at the Se sites. Apparently, these spectrum data indicate that all the Se sites in the unit cell are essentially identical.

The sample used for the ^{77}Se-NMR measurements was grown using a standard method [22] without ^{77}Se enrichment (the natural abundance of ^{77}Se is 7.5%). The sample dimension is $a^* \times b^* \times c$ = 0.09 mm × 0.04 mm × 0.80 mm corresponding to a mass of ~ 7 μg with ~ 2.0×10^{15} ^{77}Se nuclei.

Due to the small number of spins, a small microcoil with a filling factor ~ 0.4 was used. For most acquisitions, 10^4–10^5 averages were used on a time scale of ~ 5 min for 10^4 averages. The sample and coil were rotated on a goniometer (rotation angle ϕ) whose rotation axis is along the lattice c-axis (the needle direction) and it is also perpendicular to the applied field

$\boldsymbol{H}_0$ = 9 T. According to the crystal structure of λ–(BETS)$_2$FeCl$_4$, our calculation indicates that the direction of the Se-electron p_z orbital is 76.4° from the *c*-axis. Thus the minimum angle between p_z and $\boldsymbol{H}_0$ during the rotation of the goniometer is ϕ_{min}=13.6°.

5.1.2. Temperature dependence of the ^{77}Se-NMR resonance frequency

The temperature (*T*) dependence of the ^{77}Se-NMR resonance frequency (ν) from the above experiment is shown in Fig. 8 (a). In order to understand the origin of this resonance frequency, we also plotted it as a function of the 3d-Fe^{3+} ion magnetization (M_d), which is a Brillouin function of temperature *T* and the total magnetic field (H_T) at the Fe^{3+} ions. This is shown in Fig. 8 (b), where the solid lines show the fit to the M_d.

The resonance frequency ν is counted from the center of the ^{77}Se-NMR spectrum peak (maximum). What it measures is the average of the local field in magnitude in total, including the direct hyperfine field from the conduction electrons and the indirect hyperfine field that coupled to the Fe^{3+} ions at the Lamar frequency of the ^{77}Se nuclei (see details in Section 5.1.4).

Figure 8 indicates that in the PM state above ~ 7 K at the applied field $\boldsymbol{H}_0$ = 9 T, a good fit to frequency ν (uncertainty ± 3 kHz) is obtained using

$$\nu(T, H_0) \approx a - bM_d(T, H_T), \tag{2}$$

where the fit parameters *a* = 73.221 MHz and *b* = 3.0158 [(mol.Fe/emu) .MHz].

This result is a strong indication that the temperature *T* dependence of the^{77}Se-NMR resonance frequency ν is dominated by the hyperfine field from the Fe^{3+} ion magnetization M_d.

It is important to notice that the sign of the contribution from M_d is negative in Eq. (2). Thus, this also indicates that the hyperfine field from the Fe^{3+} ion magnetization is negative, i.e., opposite to applied magnetic field $\boldsymbol{H}_0$, as needed for the Jaccarino-Peter compensation mechanism.

Now, to verify to validity of the Jaccarino-Peter mechanism, we need to find the field from the 3d Fe^{3+} ions at the Se π-electrons is (i.e., the π-d exchange field $\boldsymbol{H}_{\pi d}$) which is the central goal of our ^{77}Se-NMR measurements.

According to the *H-T* phase diagram of λ–(BETS)$_2$FeCl$_4$ [Fig. 6 (c)], the magnitude of $\boldsymbol{H}_{\pi d}$ = 33 T (tesla) at temperature *T* = 5 K.

5.1.3. Angular dependence of the ^{77}Se-NMR resonance frequency

The angular dependence of the ^{77}Se-NMR resonance frequency ν from our experiments is shown in Fig. 9, which is plotted as a function of angle ϕ at several temperatures. The angle ϕ basically describes the alignment direction of the applied magnetic field $\boldsymbol{H}_0$ relative to the sample lattice.

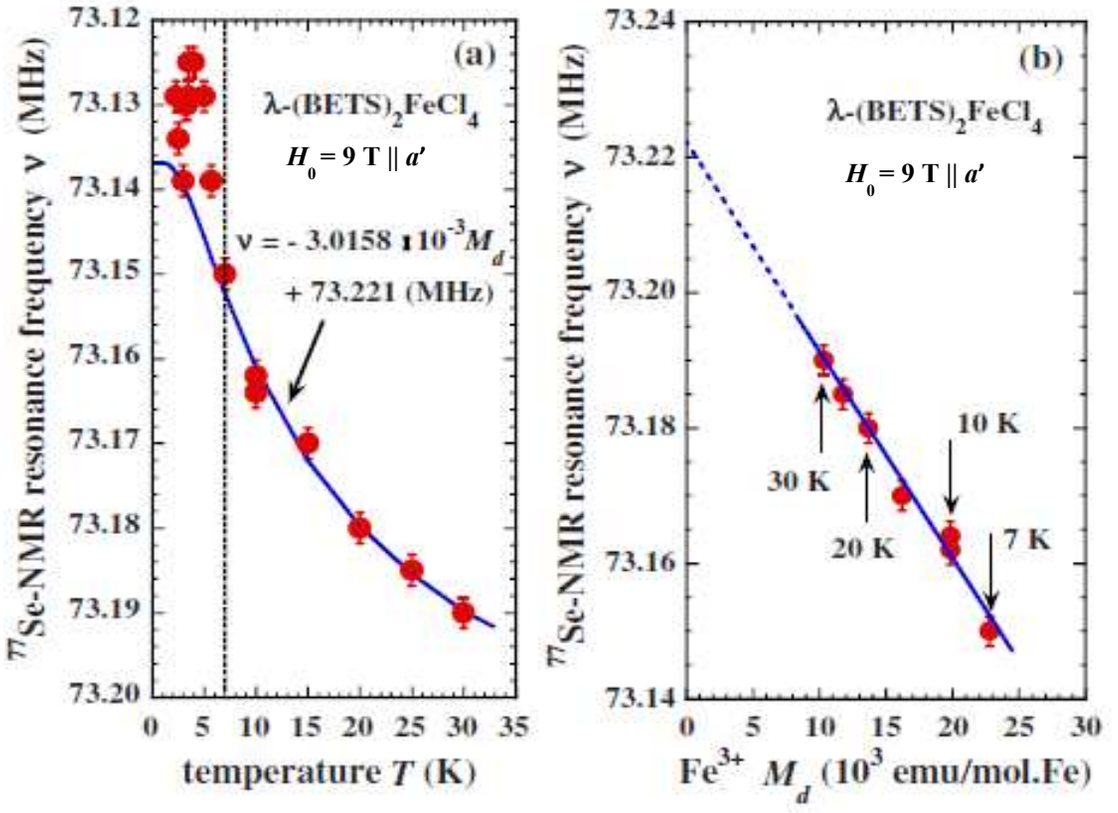

Figure 8. (a) ^{77}Se-NMR frequency shift as a function of temperature, and (b) ^{77}Se-NMR frequency shift vs the Fe^{3+} magnetization, with applied magnetic field B_0 = 9 T || a' in λ–$(BETS)_2FeCl_4$ [23].

To understand the complexity of these sets of data, we need clarify the angle ϕ first as there are many other directions involved here as well. First, the crystal lattice has its a, b and c axes which have their own fixed directions. Second, the z component of the BETS molecule π-electron orbital moment, p_z, also has a fixed direction, which is perpendicular to the BETS molecule Se-C-S loop plane. Third, there is a direction of sample rotation which is along c (the needle direction) in the applied magnetic field $\boldsymbol{H}_0$.

To distinguish each of these directions, we used the Cartesian xyz reference system and choose the reference z axis to be parallel to the lattice c axis, then the direction of p_z is determined to have angle 76.4° from the c axis through our calculation according to the X-ray data of λ–$(BETS)_2FeCl_4$. All these are clearly drawn as that shown in the inset of Fig. 9.

Thus during a sample rotation the direction of $\boldsymbol{H}_0$ is always in the xy-plane, where x-axis is chosen to be in the c-p_z plane, and the angle ϕ is counted from the x-axis.

Therefore, an angle ϕ = 0° corresponds to $\boldsymbol{H}_0$ to be in the c-p_z plane with the smallest angle between $\boldsymbol{H}_0$ and p_z as ϕ_{min}= 13.6° as mentioned in Section 5.1.1.

Based on these data shown in Figs. 8 - 9, we can determine the magnitude of the π-d exchange field $\boldsymbol{H}_{\pi d}$ precisely.

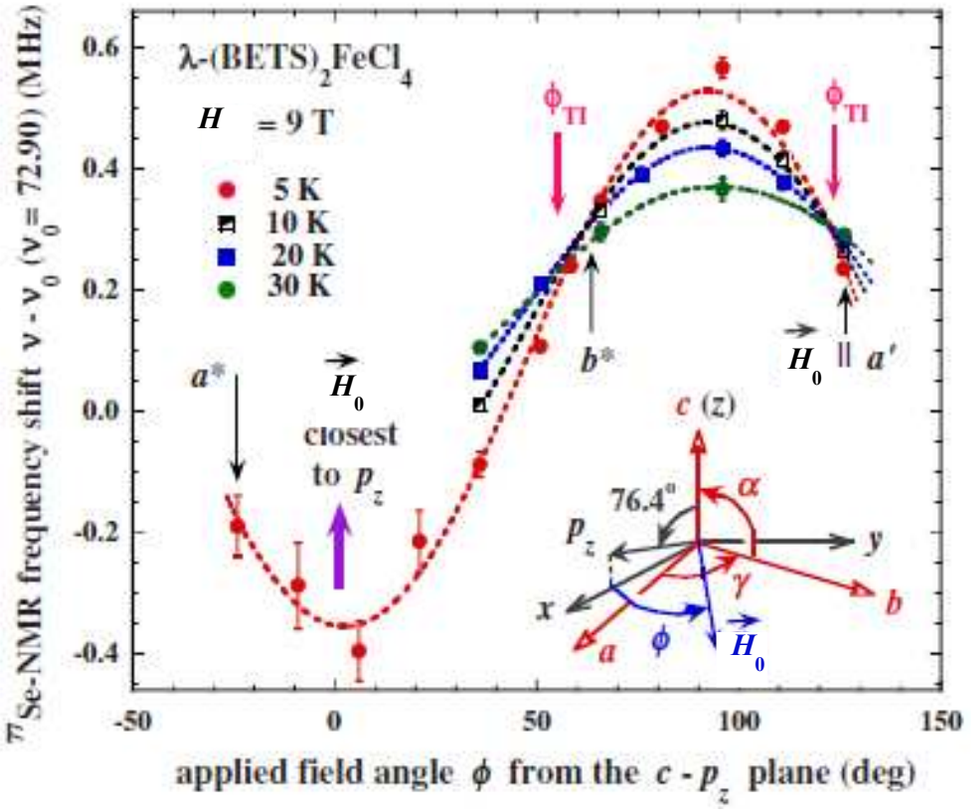

Figure 9. Angular dependence of the ^{77}Se-NMR resonance frequency ν plotted at several temperatures for the rotation of $H_0 = 9$ T about the c axis in λ–(BETS)$_2$FeCl$_4$ [23].

5.1.4. Determination of the π-d exchange field (between the Se-π and Fe^{3+}-d electrons)

From the theory of NMR [25], we can express the contributions to the Hamiltonian (H_I) of the ^{77}Se nuclear spins as

$$H_I \approx H_{IZ} + H_{I\pi}^{hf} + H_{Id}^{hf} + H_d^{dip}, \tag{3}$$

where H_{IZ} is from the Zeeman contribution due the applied magnetic field, $H_{I\pi}^{hf}$ is from the direct hyperfine coupling of the ^{77}Se nucleus to the BETS π-electrons, while H_{Id}^{hf} is from the indirect hyperfine coupling via the π-electrons to the 3*d* Fe^{3+} ion spins, and the last term H_d^{dip} is from the dipolar coupling to the Fe^{3+} spins.

The π-d exchange field $\boldsymbol{H}_{\pi d}$ comes from H_{Id}^{hf}, and the term H_d^{dip} produces dipolar field $\boldsymbol{H}_{\rm dip}$. We calculated $\boldsymbol{H}_{\rm dip}$ from the summation of the near dipole, the bulk demagnetization and the Lorentz contributions. The cartoon of the π-d exchange interaction for the Jaccarino-Peter mechanism and the sample rotation direction in the magnetic field are shown in Fig. 10.

From Eq. (3) the corresponding ^{77}Se NMR resonance frequency ν is

$$\begin{aligned}&\nu(\phi', H_0, T)\\&= {}^{77}\gamma\left[H_0 + H_{dip}(H_0, T)\right]\left[1 + K_c + K_s(\phi')\right] + {}^{77}\gamma\, K_s(\phi') H_{\pi d}(H_0, T),\end{aligned} \tag{4}$$

where ϕ' is the angle between $\boldsymbol{H}_0$ and the p_z directions, and K_c and $K_s(\phi')$ are, respectively, the chemical shift and the Knight shift of the BETS Se π-electrons.

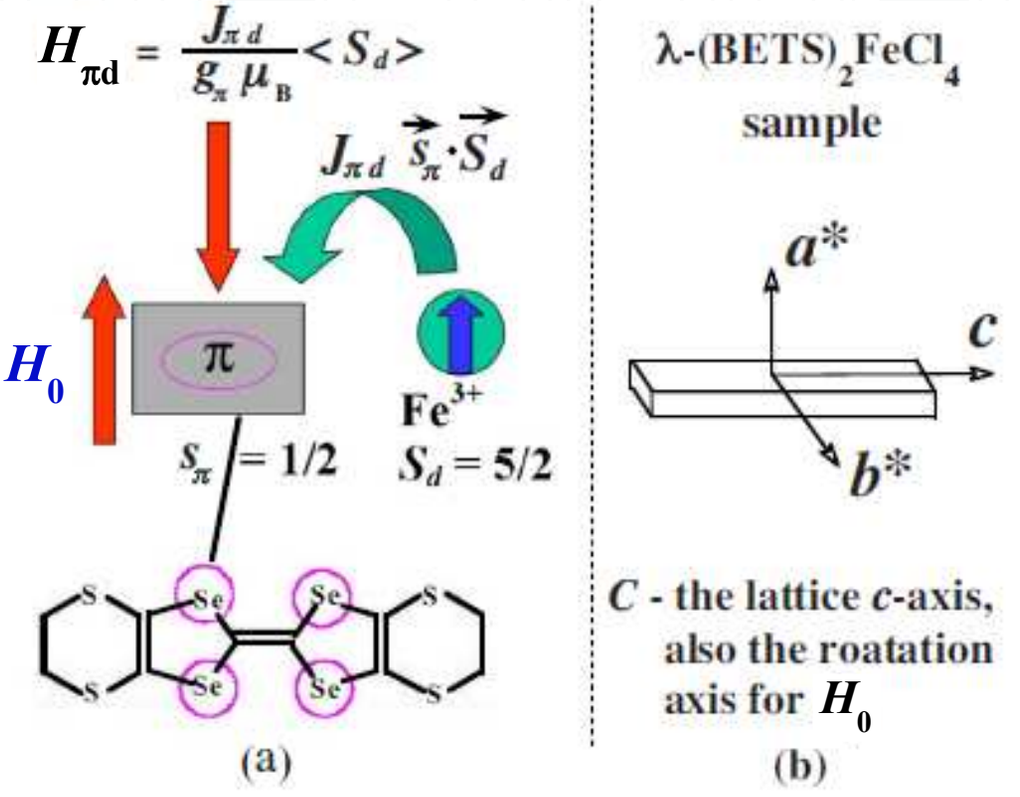

Figure 10. (a) Cartoon of the interactions for the Jaccarino-Peter mechanism. (b) Sketch of the sample rotation direction used for the ^{77}Se-NMR measurements [23].

Here,

$$K_s(\phi') = K_{iso} + K_{an}(\phi') = K_{iso} + K_{ax}\left[3\cos^2\phi\cos^2\phi_{\min} - 1\right], \tag{5}$$

where K_{iso} and K_{an} (ϕ') are the isotropic and axial (anisotropic) parts of the Knight shift, respectively. $K_{iso(ax)}$ is a constant determined by the isotropic (axial) hyperfine field produced by the $4p_\pi$ spin polarization of the BETS Se π-electrons [26].

The dashed lines in Fig. 8 are the fit to Eqs. (4) – (5). The gyromagnetic ratio of Se nucleus is $^{77}\gamma$ = 8.131 MHz/T. The value of K_{ax}= 15.3 × 10^{-4} can be obtained precisely from the BETS molecule magnetic susceptibility and the π-electron spin polarization configuration [20, 26]. From the fit, now we can obtain the value of the π-d exchange field $\boldsymbol{H}_{\pi d}$.

Alternatively, for better accuracy we obtained the following expression for the π-d exchange field $\boldsymbol{H}_{\pi d}$ from Eqs. (4) – (5) to be,

$$H_{\pi d}(H_0, T_0) = \frac{\Delta\nu(T_0, \phi_1, \phi_2)}{^{77}\gamma \Delta K_{an}(\phi_1, \phi_2)} - \frac{H_{dip}(\phi_1) - H_{dip}(\phi_2)}{\Delta K_{an}(\phi_1, \phi_2)} - H_0. \quad (6)$$

Thus from the data T_0 = 5 K, ϕ_1 = 90°, and ϕ_2 = 0° as shown from Fig. 8, it gives $\Delta\nu(5K,\ 90^\circ,\ 0^\circ) =$ 880 ± 26 kHz, and $\Delta K_{an}(90^\circ,\ 0^\circ) = 4.42\times10^{-3}$. The value of $H_{dip}(90^\circ) - H_{dip}(0^\circ) = 3.63\times10^{-3}$ T is calculated with H_0 = 9.0006 T. With these values we obtained $H_{\pi d}$ = (- 32.7 ± 1.5) T at temperature T = 5 K and applied field H_0 = 9 T. This is very close to the expected value of −33 T obtained from the electrical resistivity measurement [27, 28] and the theoretical estimate [29].

If the applied field is H_0 = 33 T, by using our modified Brillouin function with the average of the Fe^{3+} spins, we expected the value of the $H_{\pi d}$ (33 T, 5 K) = (- 34.3 ± 2.4) T.

This large value of negative π-d exchange field felt by the Se conduction electrons obtained from our NMR measurements verifies the effectiveness of the Jaccarino-Peter compensation mechanism responsible for the magnetic-field-induced superconductivity in the quasi-2D superconductor λ–(BETS)$_2$FeCl$_4$.

6. Summary

We have presented briefly the information about the field-induced-superconductors including the theories explaining the mechanisms for the field-induced superconductivity. We also summarized our ^{77}Se-NMR studies in a single crystal of the field-induced superconductor λ–(BETS)$_2$FeCl$_4$, while most of our detailed research NMR work including both proton NMR and ^{77}Se-NMR were reported in refs.[20, 23, 24].

Our ^{77}Se-NMR experiments revealed large value of negative π-d exchange field ($H_{\pi d} \approx$ 33 T at 5 K) from the negative exchange interaction between the large 3d-Fe^{3+} ions spins and BETS conduction electron spins existing in the material. This result directly verified the effectiveness of the Jaccarino-Peter compensation mechanism responsible for the magnetic-field-induced superconductivity in this quasi-2D superconductor λ–(BETS)$_2$FeCl$_4$.

Future high field NMR experiments ($H_0 \geq$ 30 T) would be of interest, and NMR measurements with the alignment of applied magnetic field along the *c*-axis and sample rotation in the *ac*-plane (conducting plane) would further improve our understanding of this novel field-induced superconductor.

Author details

Guoqing Wu
Department of Physics, University of West Florida, USA

W. Gilbert Clark
Department of Physics and Astronomy, University of California, Los Angeles, USA

Acknowledgement

We are grateful to Prof. S. E. Brown at UCLA for helpful discussions and help with the NMR experiments. We also thank other coauthors J. S. Brooks, A. Kobayashi, and H. Kobayashi for our detailed ^{77}Se-NMR work published in ref. [23].

7. References

[1] Clogston, A. M., Upper limit for the critical field in hard superconductors, Phys. Rev. Lett. 15, 266 (1962).
[2] Chandrasekhar, B. S., A note on the maximum critical field of high-field superconductors. Appl. Phys. Lett. 1, 7 (1962).
[3] Tinkham, M., *Introduction to Superconductivity* (McGraw-Hill, New York, 1975).
[4] Uji, S., Shinagawa, S., Terashima, T., Yakabe, T., Terai, Y., Tokumoto, M., Kobayashi, A., Tanaka, H., Kobayashi, H., Magnetic-field-induced superconductivity in a two-dimensional organic conductor, Nature (London) 410, 908 (2001).
[5] Meul, H. W., Rossel, C., Decroux, M., et al., Observation of Magnetic-Field-Induced Superconductivity, Phys. Rev. Lett. 53, 497 (1984).
[6] Jaccarino, V. and Peter, M., Ultra-High-Field Superconductivity, Phys. Rev. Lett. 9, 290 (1962).
[7] Maekawa, S. and Tachiki, M., Superconductivity phase transition in rare-earth compounds. Phys. Rev. B 18, 4688 (1978).
[8] Uji, S., Kobayashi, H., Balicas, L. and Brooks, J. S., Superconductivity in an Organic Conductor Stabilized by a High Magnetic Field, Advanced Materials 14, 243 (2002).
[9] Kobayashi, H., Kobayashi, A., Cassoux, P., BETS as a source of molecular magnetic superconductors (BETS = bis(ethylenedithio)tetraselenafulvalene), Chem. Soc. Rev. 29, 325 (2000).
[10] Blonder, G. E., Tinkham, M. and K.lapwijk T. M., Transition from metallic to tunneling regimes in superconducting microconstrictions: Excess current, charge imbalance, and supercurrent conversion, Phys. Rev. B 25, 4515 (1982).
[11] Tian, M. L., Kumar, N., Xu, S. Y., Wang, J. G., Kurtz, J. S. and Chan, M. H. W., Phys. Rev. Lett. 95, 076802 (2005).
[12] Santhanam, P., Umbach, C. P. and Chi, C. C., Negative magnetoresistance in small superconducting loops and wires, Phys. Rev. B 40, 11392 (1989).
[13] Xiong, P., Herzog, A. V. and Dynes, R. C., Negative Magnetoresistance in Homogeneous Amorphous Superconducting Pb Wires, Phys. Rev. Lett. 78, 927 (1997).

[14] Rogachev, A., Wei, T.-C., Pekker, D., Bollinger, A. T., Goldbart, P. M. and Bezryadin, A., Magnetic-Field Enhancement of Superconductivity in Ultranarrow Wires, Phys. Rev. Lett. 97, 137001 (2006).

[15] Agassi, A. and Cullen, J. R., Current-phase relation in an intermediately coupled superconductor-superconductor junction, Phys. Rev.B, 54, 10112 (1996)

[16] Chen, Y. S., Snyder, S. D. and Goldman, A. M., Magnetic-Field-Induced Superconducting State in Zn Nanowires Driven in the Normal State by an Electric Current, Phys. Rev. Lett. 103, 127002 (2009).

[17] Fu, H. C., Seidel, A., Clarke, J. and Lee, D.-H., Stabilizing Superconductivity in Nanowires by Coupling to Dissipative Environments, Phys. Rev. Lett. 96, 157005 (2006); Sehmid, A., Diffusion and Localization in a Dissipative Quantum System, Phys. Rev. Lett. 51, 1506 (1983).

[18] Kivelson, S. A. and Spivak, B. Z., Aharonov-Bohm oscillations with period hc /4e and negative magnetoresistance in dirty superconductors, Phys. Rev. B 45, 10490 (1992).

[19] Kobayashi, A., Udagawa, T., Tomita, H., Naito, T., Kobayashi, H., New organic metals based on BETS compounds with MX_4^- anions (BETS = bis(ethylenedithio) tetraselenafulvalene; M = Ga, Fe, In; X = Cl, Br), Chem. Lett. 22, 2179 (1993).

[20] Wu, Guoqing, Ranin, P., Clark, W. G., Brown, S. E., Balicas, L. and Montgomery, L. K., Proton NMR measurements of the local magnetic field in the paramagnetic metal and antiferromagnetic insulator phases of λ–$(BETS)_2FeCl_4$, Physical Review B 74, 064428 (2006).

[21] Kobayashi, H., Fujiwara, F., Fujiwara, H., Tanaka, H., Akutsu, H., Tamura, I., Otsuka, T., Kobayashi, A., Tokumoto, M. and Cassoux, P., Development and physical properties of magnetic organic superconductors based on BETS molecules [BETS=Bis(ethylenedithio)tetraselenafulvalene], J. Phys. Chem. Solids 63, 1235 (2002).

[22] Kobayashi, H., Tomita, H., Naito, T., Kobayashi, A., Sakai, F., Watanabe, T. and Cassoux, P., New BETS Conductors with Magnetic Anions (BETS) bis(ethylenedithio)tetraselenafulvalene), J. Am. Chem. Soc. 118, 368 (1996).

[23] Wu, Guoqing, Clark, W. G., Brown, S. E., Brooks, J. S., Kobayashi, A. and Kobayashi, H., ^{77}Se-NMR measurements of the π-d exchange field in the organic superconductor λ–$(BETS)_2FeCl_4$, Phys. Rev. B 76, 132510 (2007).

[24] Wu, Guoqing, Ranin, P., Gaidos, G., Clark, W. G., Brown, S. E., Balicas, L. and Montgomery, L. K., ^{1}H-NMR spin-echo measurements of the spin dynamic properties in lambda-$(BETS)_2FeCl_4$, Phys. Rev. B 75, 174416 (2007).

[25] Slichter, C. P., *Principles of Magnetic Resonance*, 3rd ed. (Springer, Berlin, 1989).

[26] Takagi, S., *et al*., ^{77}Se NMR Evidence for the Development of Antiferro-magnetic Spin Fluctuations of π-Electrons in λ-$(BETS)_2GaCl_4$, J. Phys. Soc. Jpn. 72, 483 (2003).

[27] Balicas, L., *et al*., Superconductivity in an Organic Insulator at Very High Magnetic Fields, Phys. Rev. Lett. 87, 067002 (2001).

[28] Balicas, L., *et al*., Pressure-induced enhancement of the transition temperature of the magnetic-field-induced superconducting state in λ-$(BETS)_2FeCl_4$, Phys. Rev. B 70, 092508 (2004).

[29] Mori, T. and Katsuhara, Estimation of πd-Interactions in Organic Conductors Including Magnetic Anions, M., J. Phys. Soc. Jpn. 71, 826 (2002).

IntechOpen